NJC

Accepted Manuscript

New Journal of Chemistry

ARTICLE

Donor–acceptor type polymers containing 2,3-bis(2-pyridyl)-5,8-dibromoquinoxaline acceptor and different thiophenes donors: Electrochemical, spectroelectrochemistry and electrochromic properties

Shuang Chen[1,2], Di Zhang[1,2], Min Wang[2], Lingqian Kong[2], Jinsheng Zhao[2]*

Three donor-accept type π-conjugated polymers, poly [2,3-di(2-pyridyl)-5,8-bis(2-thienyl) quinoxaline] (PPTQ), poly[2,3-di(2-pyridyl)-5,8-bis(2-(3-butylthiophen)) quinoxaline] (PPBTQ) and poly[2,3-di(2-pyridyl)-5,8-bis(2-(3,4-ethylenedioxythiophene)) quinoxaline] (PETQ), containing 2,3-di (2-pyridyl) quinoxaline moiety in the backbone as the acceptor unit and different thiophene derivatives as donor unites were synthesized electrochemically. Characterizations of the corresponding polymers were conducted by cyclic voltammetry (CV), UV-vis-NIR spectroscopy and scanning electron microscopy (SEM). Spectroelectrochemistry and electrochemical analyses demonstrated that all three polymers can undergo both p- and n-type doping process. PPTQ exhibits purple red in the reduced state, violet blue in the neutral state, and gray blue in the oxidation state. PPBTQ exhibits red in the reduced state, light steel blue in the neutral state, and dark slate blue in the oxidation state. PPETQ exhibits green color in the reduced state, yellow color in the neutral state, and colorless highly transmissive state in the oxidation state. PPETQ and PPBTQ revealed excellent optical contrasts of 80.3% and 78.2%, respectively in the NIR region. Outstanding optical contrasts in the NIR region, high stability and fast switching times make these polymers excellent candidates for NIR device applications.

Introduction

The organic π–conjugated polymers have caused extensive attention over the time after their discovery since they offer great potential for advanced technological applications, such as electrochromic devices[1], light emitting diodes and field effect transistors etc[2-5]. Electrochromic (EC) polymers are concisely defined as that polymers can reversibly change color by altering its redox states. And creating such kinds of electrochromic materials with low band gaps, high optical contrasts, fast response times, superior coloration efficiencies, low costs and easy processing is always what all the researchers continually seek[6].

The cathodically coloring polymers (polymers with colored reduced and transmissive oxidized states), such as polymers with neutral green and oxidation transmissive properties, are of great importance for the fabrication of EC device such as smart windows[7]. The polymers with low band gaps usually produce cathodically coloring materials because of the lower energy transition in the doped state[8]. Low band gap donor-acceptor polymers are of interest owing to the possibility of attaining multiple redox states (p-type or n-type doping) in a small

potential window. This is due to the placement of the valence band relative to the conduction band[9]. By alternating electron rich (donor, D) and electron poor (acceptor, A) moieties in the main chain of the D-A type polymers, it is possible to accurately tune the optical band gap and redox potentials that control the coverage of optical absorption[10].

It is well known that aromatic compounds with electron-withdrawing imine nitrogens (C=N) are typical acceptor-type building blocks[11,12]. Quinoxaline derivatives as this kind of organic molecules combined in the D-A type polymers as the acceptor moiety have attracted increasing interests in recent years. Besides, the quinoxaline-fused ring can ensure a rigid coplanar backbone and a highly extended π-electron system with strong π-stacking[13], which are crucial requirement for the high-performance electrochromic materials. Additionally, different thiophene-based derivatives as a series of donor moieties have gained much attention during the past decades, owing to the variation of the optical and electronic properties by light structural modification[14,15]. Therefore the combination of different thiophene derivatives and quinoxaline compound is considered as a promising way to obtain new polymers with excellent electrochemical properties[16]. Poly(2,3-bis(3,4-

bis(decyloxy)phenyl)-5,8-bis(2,3-dihydrothieno[3,4-b][1,4]dioxin-5-yl)quinoxaline) (PDOPEQ) as an example of quinoxaline based polymer revealed processable green-to-transmissive electrochromism with superior optical contrasts and fast switching times, which make this polymer unique among numerous electrochromic conjugated polymers[17]. The synthesis of conjugated polymers with various optical band gaps and color changes is a major driving force for the development of electrochromic materials[18]. During the course of preparing the D-A type electrochromic materials, the change of the structure type of the acceptor unit with the same donor unit can effectively tune the electrochromic properties of the polymers, including the optical band gaps and the color changes[19]. Recently, a new conjugated polymer with donor-acceptor architectures based on alternating 1,4-divinyl-2,5-dioctyloxybenzene and 5,8-(2,3-dipyridyl)-quinoxaline was synthesized and characterized with respect to its properties as polymer solar cell materials and trinitrotoluene sensing materials[20]. However, to the best of our knowledge, there are no any reports concerning the synthesis and characterizations of the D-A type polymers containing the alternating 5,8-(2,3-dipyridyl)-quinoxaline units and the bithiophene units, although this type of conjugated polymers usually have excellent electrochromic properties including fast switching times, outstanding stabilities, and high contrast ratios in the visible and near infrared regions.

Based on the consideration above, three novel monomers including 2,3-di(2-pyridyl)-5,8-bis(2-thienyl) quinoxaline (PTQ), 2,3-di(2-pyridyl)-5,8-bis(3-butylthiophen-2-yl)) quinoxaline (PBTQ) and 2,3-di(2-pyridyl)-5,8-bis(2-(3,4-ethylenedioxythienyl)) quinoxaline (PETQ) were synthesized by Stille coupling reaction in advance. And then, the monomers were electrochemically synthesized to their corresponding polymers including PPTQ, PPBTQ and PPETQ. The electrochemical and electrochromic properties of these polymers were also described. It was interesting to find that the slight structural change of three polymers could give rise to significant difference of electrochemical and color change. Through the analysis of the data results, the strong ethylenedioxythiophene electron-donating group can successfully tailor the electrochromic properties by combining a low monomer oxidation potential and a narrow band gap as well as the high electrical conductivity. In addition, PPETQ showed a green color in the reduced state, a deep yellow color in the neutral state and a highly transmissive oxidized state, which are not yet reported so far.

All three polymers exhibited high optical contrasts, reasonable coloration efficiencies (CE) and satisfactory response times. What's more, the presentation of redox peaks and variation of the spectroelectrochemistry at negative potentials proves the real existence of n-doping process of all three polymers. These characteristics make the polymers of important application prospects in the field of smart electrochromism.

Experimental

Materials

3,4-ethylenedioxythiophene (EDOT) (99%), thiophene (99%), 3-butylthiophene (99%), and dibromo-2,1,3-benzothiadiazole (98%) were all purchased from Puyang Huicheng Electronic Material Co., Ltd. and used as received. P-toluenesulfonicacid (PTSA, 98%), sodium borohydride (NaBH$_4$, 98%), bis(triphenylphosphine) dichloropalladium (Pd(PPh$_3$)$_2$Cl$_2$), anhydrous ethyl alcohol (EtOH,

99.9%), 2,2'-pyridil (98%), n-butyllithium (2.5 M) and chlorotributyltin (97%) were all purchased from Aladdin Chemical Co., Ltd. China. Commercial high-performance liquid chromatography grade acetonitrile (ACN, Tedia Company, INC., USA) and dichloromethane (DCM, Sinopharm Chemical Reagent Co., Ltd., China) were used as received without further purification. Tetra-n-butylammonium hexafluorophosphate (TBAPF$_6$, Alfa Aesar, 98%) was dried in vacuum at 60 ºC for 24 hours before use. Tetrahydrofuran (THF, Tianjin windship chemistry Technological Co., Ltd., China) was distilled over Na in the presence of benzophenone prior to use. Indium-tin-oxide-coated (ITO) glass (sheet resistance : < 10 Ω □$^{-1}$, purchased from Shenzhen CSG Display Technologies, China) was washed with ethanol, acetone and deionized water successively under ultrasonic, and then dried by N$_2$ flow.

Synthesis procedure

3,6-dibromo-1,2-phenylenediamine and 2,3-Bis(2-pyridyl)-5,8-dibrom oquinoxaline.

5.75 g (19.56 mmol) of 4,7-Dibromo-2,1,3-benzothiadiazole and 250 ml of anhydrous ethyl alcohol were added into round-bottom flask, meanwhile, 16.5 g (436 mmol) of NaBH$_4$ was added in three installments gradually (at 0 h, 8 h and 16 h, respectively). The solution was stirred in ice bath at 0 °C for 48 h. After the reaction, the mixture was pulled into distilled water, stirring and filtering to get white 3,6-dibromo-1,2-phenylenediamine solid (3.38 g, 65%)[21]. ^{1}H-NMR (400 MHz, CDCl$_3$; δ/ppm): 6.75 (s, 2H), 3.83 (s, 4H). ^{13}C-NMR (100 MHz, CDCl$_3$; δ/ppm): 133.74, 123.37, 109.70.

A solution of 2,3-diamino-1,4-dibromobenzene (1.03 g, 3.8 mmol), 2,2'-bipyridil (0.806 g, 3.8 mmol) and 6 mL of acetic acid in 25 mL of ethanol was heated to reflux for 3 h, then cooled to 0 °C. The formed precipitate was isolated by filtration and washed with ethanol to afford 1.16 g of 2,3-diamino-1,4-dibromobenzene as yellow solid[20]. Yield 70%, mp: 251-253 °C. ^{1}H NMR (CDCl$_3$; δ/ppm): 7.25-7.28 (d, 2H), 7.87-7.98 (d, 6H), 8.26-8.32 (m, 2H). ^{13}C NMR (CDCl$_3$; δ/ppm): 123.4, 123.8, 125.4, 133.6, 136.9, 148.2, 153.4, 156.5. Anal. Calcd. (%) for C$_{18}$H$_{10}$Br$_2$N$_4$ (442.11): C, 48.90; H, 2.28; N, 12.67. Found (%): C, 48.01; H, 2.47; N, 11.53.

PTQ, PBTQ and PETQ

As shown in Scheme 1, PTQ, PBTQ and PETQ were synthesized via Stille cross coupling reaction. Tributylstannane compounds were prepared according to previous literature methods[17]. 2,3-Bis(2-pyridyl)-5,8-dibromoquinoxaline (1.768 g, 4 mmol) and the excessive corresponding tributylstannane compounds (16 mmol) were dissolved in dry THF (60 ml). Pd(PPh$_3$)$_2$Cl$_2$ (0.28 g, 0.4 mmol) used as the catalytic was also added in the solution. The solution was stirred under nitrogen atmosphere for 30 min at room temperature. Raising the temperature immediately until the solution was refluxed. The mixture was refluxed for 24 h, and then concentrated on the rotary evaporator. The reaction mixture for the PTQ monomer was purified using column chromatography on silica gel, in which n-hexane-dichloromethane (2:1 by volume) was the eluent. The purified product PTQ is yellow solid. ^{1}H NMR (CDCl$_3$, 400 MHz, ppm): δ= 8.46 (d, 2H, ArH), 8.30 (d, 2H, ArH), 8.20 (s, 2H, ArH), 7.96 (t, 2H, ArH), 7.88 (d, 2H,), 7.55 (d, 2H), 7.26(t, 2ArH), 7.21(t, 2H). ^{13}C NMR (CDCl$_3$, 101 MHz, ppm): δ= 157.65, 151.39, 148.31, 143.08, 138.92, 137.36, 136.94, 131.781, 129.03, 127.85, 126.89, 124.79,

123.20 (see Supporting Information Fig. S1). Anal. Calcd. (%) for $C_{26}H_{16}N_4S_2$: C, 69.62; H, 3.60; N, 12.48; S, 14.30. Found: C, 69.57; H, 3.59; N, 12.53; S, 14.31. mp, 176.5 °C. HRMS (m/z, EI[+]) calcd for $C_{26}H_{16}N_4S_2$, 448.56, found 448.23.

The reaction mixture for the PBTQ monomer was purified using column chromatography on silica gel, in which n-hexane-dichloromethane (3:1 by volume) was the eluent. The purified product PBTQ is orange yellow solid. ^{1}H NMR (CDCl$_3$, 400 MHz, ppm): δ= 8.46 (d, 2H, ArH) 8.29 (d, 2H, ArH) 8.14 (s, 2H, ArH), 7.94 (t, 2H, ArH), 7.72 (d, 2H,), 7.25 (t, 2H, ArH), 7.1(d, 2H), 2.7 (t, 4H), 1.7 (m, 4H),1.44 (m, 4H), 0.97 (t, 6H). ^{13}C NMR (CDCl$_3$, 101 MHz, ppm): δ= 157.64, 151.12, 148.32, 143.06, 138.50, 137.35, 137.05, 131.65, 128.46, 127.69, 124.83, 124.15, 123.22, 33.01, 30.48, 22.69, 14.25 (see Supporting Information Fig. S2). Anal. Calcd. (%) for $C_{30}H_{20}N_4O_4S_2$: C, 63.81; H, 3.57; N, 9.92; O, 11.33; S, 11.36. Found: C, 63.49; H, 3.89; N, 9.43; O, 11.67; S, 11.52. Mp, 309.8 °C. HRMS (m/z, EI[+]) calcd for $C_{30}H_{20}N_4O_4S_2$, 564.63, found 564.56.

The reaction mixture for the PETQ monomer was purified using column chromatography on silica gel, in which n-hexane-dichloromethane (3:1 by volume) was the eluent. The purified product PETQ is red solid. ^{1}H NMR (CDCl$_3$, 400 MHz, ppm): δ= 8.67 (s, 2H, ArH), 8.48 (d, 2H, ArH), 8.28 (d, 2H, ArH), 7.94 (t, 2H, ArH), 6.57 (s, 2H), 4.36 (dd, 8H). ^{13}C NMR (CDCl$_3$, 101 MHz, ppm): δ= 157.54, 150.31, 148.23, 141.58, 140.62, 137.15, 136.96, 129.09, 128.78, 124.97, 123.03, 113.43, 103.37, 65.15, 64.53 (see Supporting Information Fig. S3). Anal. Calcd. (%) for $C_{34}H_{32}N_4S_2$: C, 72.82; H, 5.75; N, 9.99; S, 11.44. Found: C, 72.77; H, 5.87; N, 9.89; S, 11.49. mp, 135.2 °C. HRMS (m/z, EI[+]) calcd for $C_{34}H_{32}N_4S_2$, 560.77, found 560.89.
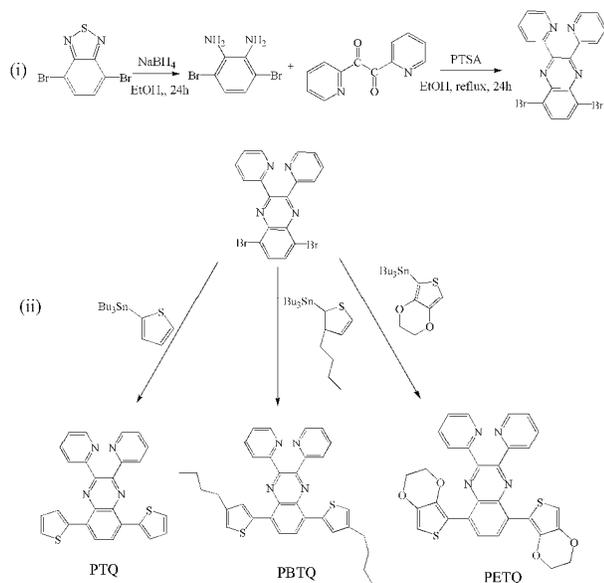
Scheme 1 Synthetic route of the monomers.

Instrumentation

^{1}H NMR and ^{13}C NMR spectra of the monomers were recorded on a Varian AMX 400 spectrometer in CDCl$_3$ at 400 MHz and chemical shifts (δ) were given relative to tetramethylsilane as the internal standard.. Scanning electron microscopy (SEM) measurements were taken by using a Hitachi SU-70 thermionic field emission SEM. UV-Vis-NIR spectra were carried out on a Varian Cary 5000 spectrophotometer under the control of a computer. Digital photographs of the polymer films were taken by a Canon Power Shot A3000 IS digital camera. Electrochemical syntheses and experiments were performed in a one-compartment cell with a CHI 760 C Electrochemical Analyzer (Shanghai Chenhua Instrument Co. China) under control of a computer. Elemental analyses are determined by a Thermo Finnigan Flash EA 1112, CHNS-O elemental analyses instrument. The thickness and surface roughness of the polymer films were recorded on a KLA-Tencor D-100 step profiler. Mass spectrometry analysis was conducted using a Bruker maXis UHR-TOF mass spectrometer.

Electrochemistry

Electrochemical syntheses and experiments were performed in an one-compartment cell with a CHI 760 C Electrochemical Analyzer (Shanghai Chenhua Instrument Co. China) under control of a computer at room temperature. The working electrode was a platinum wire with a diameter of 0.5 mm, a platinum ring worked as counter electrode, and a silver wire (Ag wire) was taken as pseudo reference electrode. The working and counter electrodes for cyclic voltammetric experiments were placed 0.5 cm apart during the experiments. All electrochemical polymerization and CV tests were taken in DCM containing 0.1 M TBAPF$_6$ as a supporting electrolyte with or without 4 mM monomers. The pseudo reference electrode was calibrated externally using a 5 mM solution of ferrocene (Fc/Fc[+]) in DCM solution containing 0.1 M TBAPF$_6$ as the electrolyte, and the half-wave potential ($E_{1/2}$) of Fc/Fc[+] measured was 0.39 V vs. Ag wire. Concerning the fact that the $E_{1/2}$ of Fc/Fc[+] measured in DCM solution containing 0.1 M TBAPF$_6$ was 0.42 V vs. SCE. Thus, the potential of Ag wire was assumed to be 0.03 V vs. SCE[10]. All of the electrochemical experiments were carried out at room temperature under nitrogen atmosphere, and taking the Ag wire as the pseudo reference electrode. Cyclic voltammetry (CV) of the polymer was carried out with the same electrode set-up in monomer-free electrolyte solution.

Spectroelectrochemistry

Spectroelectrochemical data were recorded on a Varian Cary 5000 spectrophotometer connected to a computer. A three-electrode cell assembly was used where the working electrode was an ITO glass with a surface area of 0.9×1.8 cm[2], the counter electrode was a stainless steel wire, and an Ag wire was used as pseudo reference electrode. The thickness of the polymer films grown potentiostatically on ITO was controlled by the total charge passed through the cell. The measurements were carried out in DCM solution containing 0.1 M TBAPF$_6$. Color changes were recorded with in-situ electrocolorimetric measurements under potentiostatic control using a Varian Cary 5000 spectrophotometer at color measurement mode. The standard illuminant D65 with a 2° observer at constant temperature in alight booth designed to exclude external light was used. Prior to each set of measurements, background color coordinates (x, y and z values) were taken at open-circuit, using the electrolyte solution without the polymer films under the study.

Result and discussion

Electrochemical polymerization and characterization

Electrochemical polymerization

All the polymers were polymerized on the platinum wire by cyclic voltammogram (CV) with the same potential scan rate (100 mV s^{-1}). The successive CV curves of 4 mM PTQ, PBTQ and PETQ in 0.1 M TBAPF$_6$ /DCM electrolyte are illustrated in Fig. 1. Among them, the first cycle of the CV test is ascribed oxidation of monomer. The onset oxidation potentials (E_{onset}) of PTQ and PBTQ are 1.08 and 1.06 V, respectively, with the latter is slightly lower than that of the former one, the reason for which might be the weak electron donating ability of butyl group on the thiophene ring. By comparison, the E_{onset} of PETQ is 0.83 V, being far lower than that of PTQ and PBTQ, due to the presence of strong electron donating group on donor moiety. During the successive anodic scan of the monomer, the corresponding polymer films were formed on the surface of the working electrode. As shown in Fig. 1, the CV curves of the PPTQ show a cathodic peak at around 0.93 V, while the corresponding oxidation waves are overlapped with the oxidation waves of the monomer and cannot be observed clearly. Similarly, the CV curves of PBTQ only shows a cathodic peak at around 1.0 V with the corresponding oxidation waves overlapped (Fig. S4a). However, the CV curves of PETQ present a weak oxidation peak at 0.78 V and a reduction peak at 0.38 V (Fig. S4b). In addition, the increase in the redox wave current densities implies that the amount of conducting polymers deposited on the electrode is increasing[22]. The electrochemical polymerization reaction is an electrophilic substitution which retains the aromatic structure and proceeds via a radical cation intermediate[23]. Taking the polymerization of PTQ as an example, it's polymerization mechanism by the electrochemical method was shown in Fig. S5.
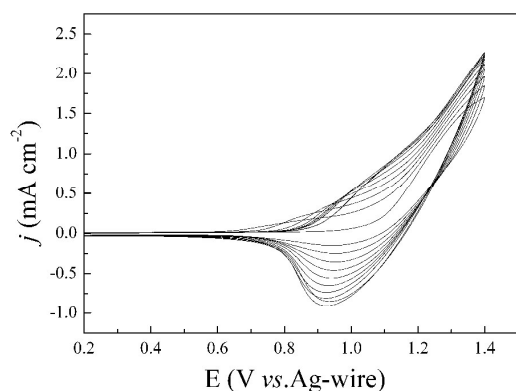

Fig. 1. Cyclic voltammogram curves of PTQ in 0.1 M TBAPF$_6$/ DCM solution at a scan rate of 100 mV s^{-1}. *j* denotes the current density. *E* denotes the potential.

Electrochemistry behavior of the polymer films

In order to make research on the electrochemical properties, three polymer films were prepared on Pt wire by sweeping the potentials three cycles. Electrochemical behaviors of the deposited polymers were investigated at different scan rates between 100 and 300 mV s^{-1} in monomer free electrolyte solution, as shown in Fig. 2. Fig. 2a shows the electrochemical behavior of the PPETQ film at different scan rates from 300 to 50 mV s^{-1} in DCM containing 0.1 M TBAPF$_6$. The polymer film exhibits a redox process between 0.42 and 0.5 V (p-doping). A couple of redox peaks with an oxidation potential of -1.26 V and a reduction potential of -1.4 V is also observed in

the reduction region, which indicates the polymer can be n-doped. What is more, the redox peaks of the n-doping/dedoping are much stronger than the p-doping/dedoping process. The results suggest that 2,3-bis(2-pyridyl)-5,8-dibromoquinoxaline is a strong electron acceptor and PPETQ is a good n-type conjugated polymer[24]. This phenomenon is also observed in other polymers including PPTQ and PPBTQ (see Supporting Information Fig. S6b and Fig. S7b) although there are no obvious n-dedoping peaks in both of the polymers. The different locations and different appearance of the oxidation and reduction peaks of the polymers reveal the influence made by different electron-rich groups. Fig. 2b and Fig. 2c shows well linear relationships between the scan rate and peak current densities (*j*) of the PPETQ polymer during the p-doping/dedoping process and the n-doping/dedoping process, which demonstrate that the film were well adhered on ITO and the electrochemical processes are non-diffusion-controlled[25]. The other two polymers including PPTQ and PPBTQ also present the similar linear relationships between the scan rates and the peak current densities (Fig. S6a and Fig. S7a)
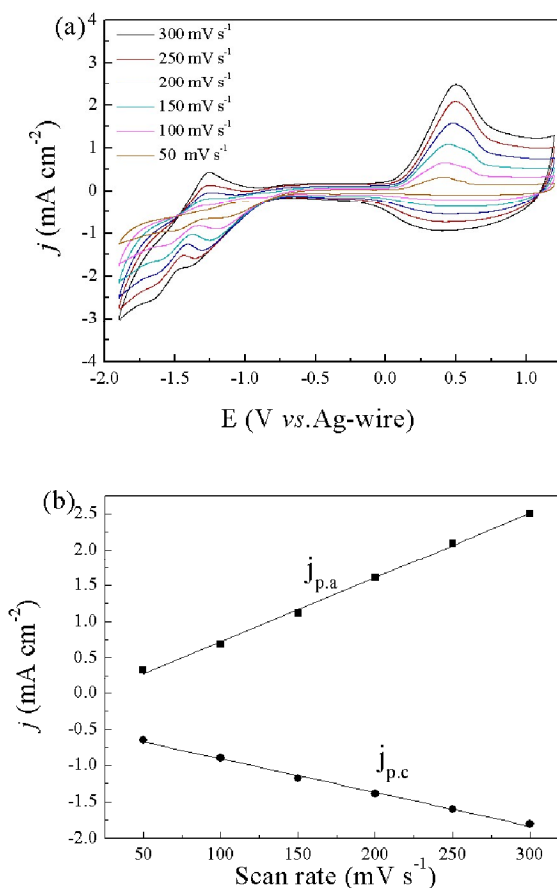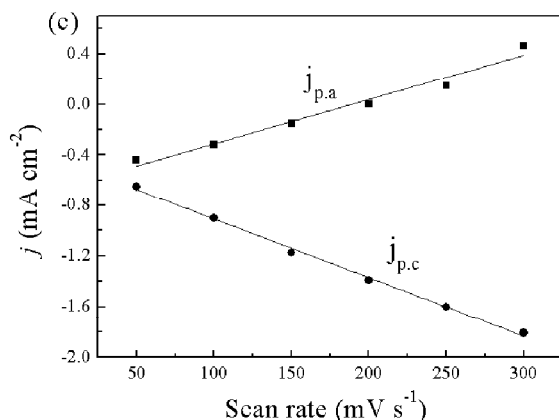
Fig. 2. (a) CV curves of PPETQ at different scan rates between 50 and 300 mV s^{-1} in the monomer-free 0.1 M TBAPF$_6$/DCM solution. (b) Scan rate dependence of the anodic and cathodic peak current densities graph of the p-doping/dedoping process. (c) Scan rate dependence of the anodic and cathodic peak current densities graph of the n-doping/dedoping process. $j_{p.a}$ and $j_{p.c}$ denote the anodic and cathodic peak current densities, respectively.

Meanwhile, the PETQ monomer is also found to exhibit a true n-doping behavior (Fig. S8). The cyclic voltammogram of the PETQ monomer was conducted between -1.7 V and +1.2 V at a scan rate of 100 mV s^{-1} in 0.1 M TBAPF$_6$/DCM solution, and the sweep is started from an initial potential of 0 V, and then a positive scan was followed by a negative scan. The PETQ exhibits an oxidation peak (or p-doping) at 0.95 V and a reduction peak (or n-doping) at −1.55 V, and the corresponding p-dedoping and n-dedoping peaks were coupled with at 0.59 V and −1.31 V, respectively. These results also support the structure of the monomer having both the strong electron-donating 3,4-ethylenedioxythiophene unit and the electron-accepting quinoxaline unit.

Morphology

Scanning electron micrographs (SEM) of polymers provide their clear surface and bulk morphologies, which are closely related to their optical and electrical properties[26]. Fig. 3 gives the SEM images of PPTQ, PPBTQ and PPETQ, which were prepared potentiostatically in the solution of 0.1 M TBAPF$_6$/DCM containing relevant monomers on ITO electrodes and dedoped before characterization. It is clearly observed that the three polymers exhibit different surface morphologies, even though the structures of them are quite similar. As shown in Fig. 3a, the PPTQ film exhibits a globular cluster structure with scattered holes between the clusters. A cauliflower structure is observed on the surface of PPBTQ film(Fig.3b). However, The PPETQ reveals coral structure with dense holes between the globules(Fig.3c). A step profiler was employed for evaluating the thickness and roughness of three polymer films deposited on the ITO electrode with a polymerization charge of $2.0×10^{-2}$ C at a surface area of 0.9 × 1.8 cm^2. The thickness profiles of three polymer films are shown in Fig.S9, and the thicknesses were measured as 827 nm, 896 nm and 625 nm for PPTQ, PPBTQ and PPETQ, respectively. The profiles of the step profiler measurements revealed that the polymer films have extremely rough surfaces

with detectable pits, which is in good agreement with the morphologies shown in the SEM images. The morphologies of the three polymers were quite different from each other, which might be an indication of the different aggregation structure of the conjugated polymers, and also be accounting for the different film thickness although the polymers had the same polymerization charges.

Optical properties of the monomers and films

As the typical feature of D-A conjugated compounds, all three monomers exhibit two characteristic absorption bands, which are assigned to the strong π-π* transition and intramolecular charge transfer band, respectively[8]. Two obvious absorption peaks can be observed at about 310 and 448 nm for PTQ, 313 and 445 nm for PBTQ, 323 and 471 nm for PETQ, respectively. Compared with PTQ and PBTQ, PETQ has an apparent red shift of the maximum absorption wavelengths due to the electron donating ability of the electron rich ethylenedioxy group, which enhances the conjugation effect of the D-A compound effectively. Similarly, there is a bit red shift of the maximum absorption wavelengths of PBTQ compared with that of PTQ due to the weak electron donating effect of the butyl group on the thiophene moiety. Furthermore, the frontier molecular orbitals of the monomers were investigated by using density functional theory (DFT) with the Gaussian 03 program at the parameters of B3LYP and 6-31+G* basis sets. The ground-state electron density distribution of the highest occupied orbital (HOMO) and lowest unoccupied molecular orbital (LUMO) are illustrated in Fig.S10. The LUMO orbitals are more localized on the electron-accepting quinoxaline moiety, while HOMO orbitals are delocalized on the electron-donating thiophene moieties, respectively. And, the results of DFT calculation also confirmed the electron transfer between the donor unit and the acceptor unit, which was accounting for the low band gaps of the D-A-D type monomers.The calculated HOMO-LUMO gaps of the monomers was found to be in the range of -2.75 eV − -2.94 eV and the data are summarized in Table 1. The highest band gap was observed for PTQ and the lowest was for PETQ, which is consistent with their strength of the electron donating abilities. Uv-vis absorption spectra of three polymer films including PPTQ, PPBTQ and PPETQ on ITO coated slide glass are shown in the inset of Fig. 4. As seen from Fig. 4, both PPTQ and PPBTQ show one absorption band in the visible region due to the π-π* transition at neutral state, with the absorption peaks at 610 and 566 nm, respectively. Different with that of PPTQ and PPBTQ, PPETQ film exhibit two separated absorption bands, with one in the visible region centered at 454 nm, and the other in the near infrared region centered at 810 nm. It is apparent that three polymers exhibit a certain amount red shift compared to the corresponding monomers as shown in Fig. 4, which indicate the formation of the long conjugated polymer chains due to the fact that the longer the wavelength of maximum absorption is, the higher the conjugation length in the polymer will be[27]. Besides, the optical band gaps (E_g) of the three polymers were calculated from its low energy absorption edges (λ_{onset}) ($E_g = 1240/\lambda_{onset}$). Based on previous results, it can be easily seen that the prepared polymer film of PPETQ has a lower band gap than that of PPTQ and PPBTQ. The E_g of the PPETQ was calculated as 1.16 eV, which was lower than that of PPBTQ (1.74 eV) and PPTQ (1.54 eV). The weak electron donating effect of the butyl group on the thiophene ring can not compensate for its repulsive steric effect on the neighboring repeat unit that decrease the effective conjugation length in the homopolymers[8]. This explained the

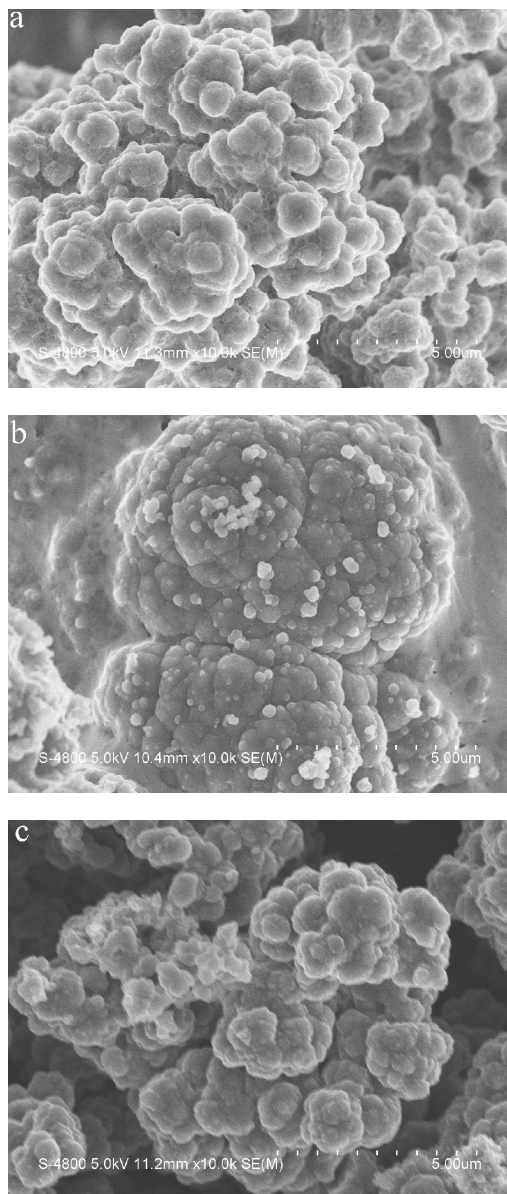fact that PPBTQ has a slightly larger band gap than that of PPTQ.

Fig. 3. SEM images of (a) PPTQ, (b) PPBTQ and (c) PPETQ films deposited potentiostatically on ITO electrode.

Table 1 summarizes the onset oxidation potential (E_{onset}), maximum absorption wavelength (λ_{max}), low energy absorption edges (λ_{onset}), HOMO and LUMO energy levels, optical band gap (E_g) values of the monomers and the corresponding polymers, as well as the calculated band gap data of the monomers from the Gaussian 03 program. HOMO energy levels of them were calculated by using the formula E_{HOMO} =−e(E_{onset} + 4.4) (vs. SCE) and LUMO energy levels (E_{LUMO}) of them were calculated by the subtraction of the optical band gap (E_g) from the HOMO levels[28].
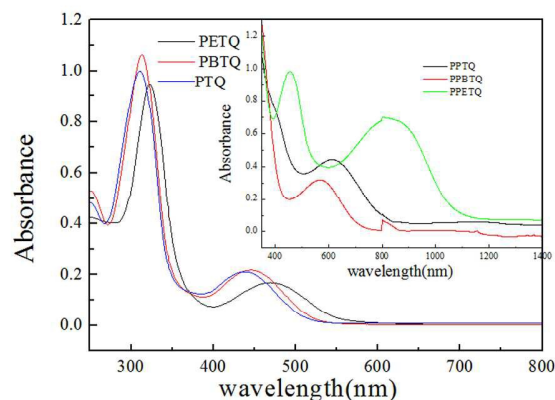

Fig. 4. UV–vis spectra of PTQ, PBTQ and PETQ in DCM. inset: absorption spectra of the corresponding polymers deposited on ITO at the neutral state.

Electrochromic properties of the polymer films

Spectroelectrochemical properties of the polymers

Spectroelectrochemistry is a useful method for studying the optical changes in the absorption spectra and the information about the electronic structures of conjugated polymers as a function of the applied potential difference[29]. Three polymer films coated ITO electrode (with the same polymerization charge of 2.0×10^{-2} C at 1.2 V for PETQ, 1.4 V for PTQ and PBTQ, respectively) were switched at different potential using a UV-Vis-NIR spectrophotometer in monomer-free 0.1 M TBAPF$_6$/DCM solution in order to obtain the in-situ UV-vis-NIR spectra (Fig. 5).

The electrochromic behavior was investigated with an UV-vis-NIR spectrometer at various applied potentials (vs. pseudomonas Ag wire reference electrode), the absorption changes in response are shown due to the localization of the redox process. And, for giving a accurate description of the color, the CIE 1931 xy chromaticity coordinates were also calculated from the in situ spectra of each film. All three polymers display similar absorption in the reduced state, with two distinct absorption bands. The high-energy peaks of PPTQ are mainly absorbing in the UV-region, with minor tailing into the visible region, limiting the contribution of the high-energy peak to the color perceived by human eye (Fig. 5a). On the other hand, the low-energy peaks, originating from the D-A interaction, have pronounced absorption in the red part of the visible region. A broader peak centered at 608 nm due to π-π* transition, partly absorbing in the yellow-brown light, resulted in a violet blue color for PPTQ (Fig. 6a) in the neutral state. The electronic band gap of the polymer, defined as the onset of the π-π* transition, was determined as 1.54 eV. During oxidation, the π-π* transition bands started to decrease and a concomitant increase was observed at 755 nm and 1230 nm due to the formation of charge carriers including polarons and bipolarons (Fig. 5a). The phenomenon of the simultaneous formation of the polarons and bipolarons could be attributed to the presence of the stable bipolaronic states on polymer backbone during the doping process. At the full oxidized state, the PPTQ presented blue-gray color due to the broad absorption centered at 755 nm, which partly absorbing the brown and red light (Fig. 5a, Fig. 6a). There are usually two transitions for the neutral states of the D-A type polymers, with one be related

with the transition from the thiophene-based valence band to its antibonding counterpart (high-energy transition), and the other be related with the transition from the thiophene-based valence band to the acceptor localized conduction band (low-energy transition). In this sence, the interactions between donor and acceptor units (their match) determine the energy and intensity of these transitions. For PPTQ, the intensity of the low energy transition was significantly smaller than that of the high energy transition, which was not centered in the visible region (with a maxima at 318 nm and not be shown completely in Fig. 5a). The lower intensity of the low-energy transition might be an indication of the weak interactions or the unsatisfactory match between the thiophene and the 5,8-(2,3-dipyridyl)-quinoxaline acceptor unit due to the weak electron donating ability of the thiophene unit.

Table 1. The onset oxidation potential (E_{onset}), maximum absorption wavelength (λ_{max}), absorption onsets wavelength (λ_{onset}), HOMO and LUMO energy levels, optical band gap (E_g) and the calculated band gap data of the monomers from the Gaussian 03 program

Compounds	E_{onset},vs. SCE (V)	λ_{onset} (nm)	$E_g{}^a$ (eV)	HOMO^b(eV)	LUMO^c (eV)	ΔE^d	HOMO^d(eV)	LUMO^d(eV)
PTQ	1.11	515	2.41	−5.51	−3.10	-2.94	-5.50	-2.56
PBTQ	1.09	521	2.38	−5.49	−3.11	-2.79	-5.31	-2.52
PETQ	0.86	552	2.25	−5.26	−3.01	-2.75	-5.12	-2.37
PPTQ	0.92	807	1.54	−5.32	−3.78	–	–	–
PPBTQ	1.04	805	1.74	-5.44	-3.70	–	–	–
PPETQ	0.11	1069	1.16	-4.51	-3.35	–	–	–

^{a} Calculated from the low energy absorption edges (λ_{onset}), $E_g = 1240/\lambda_{onset}$.
^{b} HOMO = $-e(E_{onset} + 4.4)$ (E_{onset} vs. SCE).
^{c} Calculated by the subtraction of the optical band gap from the HOMO level.
^{d} calculated by employing the Gaussian 03 program

Spectroelectrochemistry of PPBTQ shows a λ_{max} of 566 nm in the visible region due to the π-π* transition at the neutral state, which is light steel blue in color (Fig. 5b, Fig. 6b). Upon oxidation there is a decrease in the π-π* transition and the development of new transition bands at lower energy (at around 798 nm and 1364 nm, respectively), corresponding to the polaronic and bipolaronic charge carriers[30]. The full oxidized PPBTQ polymer presents a blue purple color since the presence of the significant tails of the polaronic and the bipolaronic absorption bands with a medium maxima centered at 797 nm due to the formation of the polarons (Fig. 5b, Fig. 6b). The electronic band gap of the polymer, defined as the onset of the π-π* transition, was determined as 1.74 eV. The different structures of the polymers due to the difference in donor moiety affect not only the monomer oxidation and the polymer redox couple potentials but also the maximum absorption wavelengths of the corresponding transitions. The introduction of alkyl substituent on ploymer causes steric hindrance, resulting in less order and less conjugation by the blue shift in the absorption spectra and the increase in polymer's band gap[8]. Be alike with PPTQ, there is also a minor low-energy transition obsorption for PPBTQ, which might be attributable to the weak interaction between the acceptor unit and the 3-butylthiophene unit.

Spectroelectrochemical studies of PPETQ reveal two well-separated absorption maxima centered at 448 and 808 nm, respectively, with a broad valley centered at 597 nm, which give rise to a dark yellow color in the neutral state (Fig. 5c, Fig. 6c). Compared with PPTQ and PPBTQ polymers, there are significant bathochromic shifts for both of the π-π* transition bands of PPETQ, and the intensities of two transitions are comparable with each other, which indicates the ideal match between the donor and acceptor units and the strong interactions between them. As expected, the band gap of PPETQ calculated from the onset of the π-π* transition is 1.16 eV, which is much lower than that of the PPTQ and the PPBTQ polymers. As has been known, the hybridization between the highest state of the HOMO level of the donor with the lowest state of the LUMO level of the acceptor leads to the polymer which has an ionization potential closer to donor and an electron affinity closer to the acceptor[31]. In this case, the higher HOMO level of the EDOT unit compared to that of the thiophene and the 3-butylthiophene units is the reason for the lowest band gap of the PPETQ among three polymers. The intensities of both absorption bands decreases and a new absorption band centered at 1430 nm in the NIR region arises due to the formation of charge carriers upon oxidation of the PPETQ polymer (Fig. 5c). At the full oxidation state, the loss of absorption in the visible region for the oxidized state of PPETQ is not complete and residual long wavelength absorption also remains, giving the highly transmissive polymer a slight gray hue (Fig. 5c, Fig. 6c). As mentioned previously, the necessity for a cathodically colouring yellow to transmissive electrochrome is paramount in completing the colour palette for non-emissive displays using the subtractive colour mixing theories of CMY(cyan, magenta and yellow) and RYB (red, yellow and blue).

In addition, the conducting polymers with stable negatively doped states are of high interest. The n-doping of a conjugated polymer in a n-type manner is not just an electrochemical formation of a reduced state, which is also accompanied with the introduction of charge carriers. The optical change that occurs during the n-doping of the polymer was examined to prove the introduction of a charge carrier to the conjugated system. The reductive absorption spectra of PPTQ, PPBTQ and PMFTQ are recorded at -1.4, -1.5 and -1.4 V, respectively, which are the cathodic potentials of the redox couples observed in the reduced states. For PPTQ, the absorption maxima centered at 510 nm in the visible region brought about a purple color, which indicates a significant difference from that of the neutral and p-doped states (Fig. 5a, Fig. 6a). As for PPBTQ, a well defined absorption band centered at 497 nm was found, which resulted in a red reduced state(Fig. 5b, Fig. 6b). When -1.4 V was applied for polymer PMFTQ, the film turned into a

valuable green color with two separated absorption waves at 443 and 779 nm, respectively (Fig. 5c, Fig. 6c). The electrochemical properties of the reduced states and the spectral changes that occur upon reduction proved that the n-doping process truly occurred.

To further establish the colors of the polymers, the colorimetric properties were characterized using CIEAB 1976 color space ($L*a*b*$). $L*$ can be interpreted as being the lightness variable of the material, while $a*$ and $b*$ are concerned with the red-green and yellow-blue saturation of the colour, respectively. The values of the relative $L*a*b*$ were measured in the neutral, oxidized and reduced states of the polymers and summarized in Table 2.

Table.2. The colorimetry analysis of the three polymer in reduced, neutral and oxidized states.

Polymer	E, vs (Ag wire) (V)	CIELAB 1976 ($L*a*b*$)			CIE 1931
		$L*$	$a*$	$b*$	Color coordinates
PPTQ	0	47.01	4.88	-15.80	x=0.28; y=0.28
	1.4	48.56	-11.31	-9.67	x=0. 26; y=0.31
	-1.4	60.0	8.60	7.53	x=0.35; y=0.34
PPBTQ	0	48.01	-6.78	-4.51	x=0.28; y=0.32
	1.4	36.56	11.31	-23.87	x=0.26; y=0.23
	-1.5	67.74	36.65	6.24	x=0.39; y=0.31
PPETQ	-0.2	59.57	12.21	25.16	x=0.40; y=0.38
	1.2	79.78	-4.072	7.527	x=0.32; y=0.35
	-1.4	51.61	-39.37	4.09	x=0.24; y=0.39

Electrochromic switching of PPTQ, PPBTQ and PPETQ films in solution

It is important that polymers can switch rapidly and exhibit a noteworthy color change for electrochromic applications[32]. For this purpose, double potential step chronoamperometry technique was used to investigate the switching ability of the three polymer films between its neutral and full doped state at given wavelengths[33]. The electrochromic switching behaviors of the polymers were performed at regular intervals of 5 s in a monomer free DCM solution containing 0.1 M TBAPF$_6$ as a supporting electrolyte. Fig. 7. shows the stabilities, optical contrasts and response times upon electrochromic switching of the polymer films at different wavelengths. In these studies, the optical contrast ($\Delta T\%$) of the polymer films which can be defined as the transmittance difference between the redox states was recorded at constant wavelengths[30]. Response time, another most important characteristic of electrochromic materials, is the necessary time for 95% of the full optical switch (after which the naked eye could not sense the color change)[34]. Fig. 7a shows the switching properties of PPTQ between 0.2 and 1.4 V at 1230 nm in NIR regions. The optical contrast for PPTQ was calculated as 22.8% and the switching times were 4.35 s from the reduced to the oxidized state and 3.59 s from the oxidized to the reduced state at 1230 nm. The stability of PPTQ was not very preferable since there is a moderate loose in percent transmittance contrast value after regular switching during 300 s.
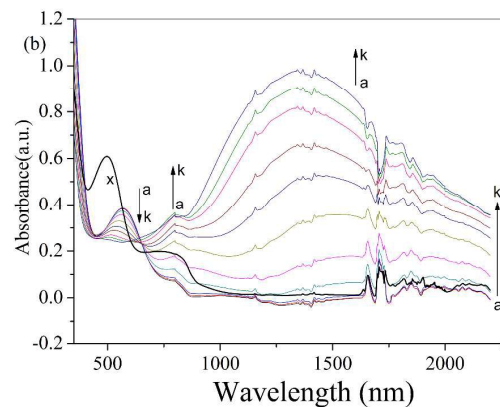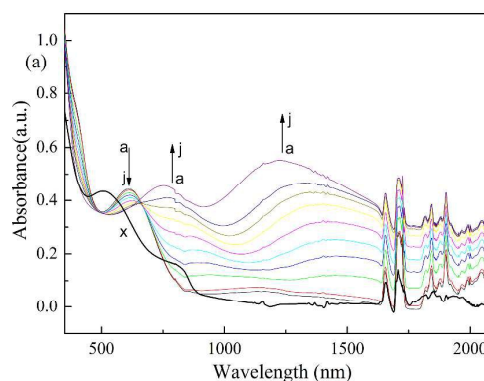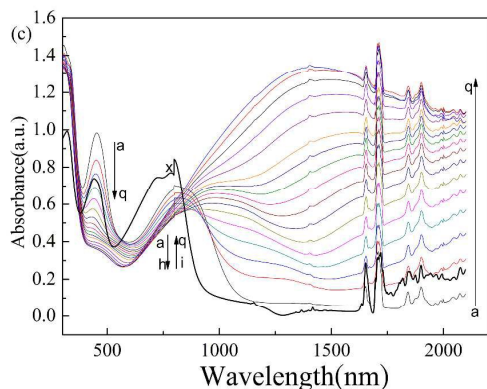
Fig. 5. [a] p-doping: spectroelectrochemistry of PPTQ film on ITO electrode in the monomer-free 0.1 M TBAPF$_6$ /DCM solution at applied potentials: (a) 0.2, (b) 0.8, (c) 0.9, (d) 0.95, (e) 1.0, (f) 1.05, (g) 1.1, (h) 1.15, (i) 1.2, (j) 1.3 V. n-doping: bold black line marked by 'x' indicates the reduction spectrum of PPTQ film at -1.7 V. [b] p-doping: spectroelectrochemistry of PPBTQ film on ITO electrode in in the monomer-free 0.1 M TBAPF$_6$ /DCM solution at applied potentials: (a) 0.2, (b) 0.8, (c) 0.85, (d) 0.90, (e) 0.925, (f) 0.95, (g) 0.975, (h) 1.0, (i) 1.05, (j) 1.1, (k) 1.2 V. n-doping: bold black line marked by 'x' indicates the reduction spectrum of PPBTQ film at -1.5 V. [c]. p-doping: spectroelectrochemistry of PPETQ film on ITO electrode in in the monomer-free 0.1 M TBAPF$_6$ /DCM solution at applied potentials: (a) -0.2, (b) 0.2, (c) 0.25, (d) 0.30, (e) 0.35, (f) 0.40, (g) 0.45, (h) 0.5, (i) 0.55, (j) 0.60, (k) 0.65, (l) 0.7 V, (m) 0.80, (n) 0.90, (o) 1.0 V, (p) 1.1, (q) 1.2 V. n-doping: bold black line marked by 'x' indicates the reduction spectrum of PPETQ film at -1.4 V.

The PPBTQ film was switched from 0.2 V to 1.3 V at 5 s step intervals while the changes in transmittance were recorded at two different wavelengths both in ultraviolet and NIR regions. The optical contrasts for PPBTQ were calculated as 16.9% at 336 nm, 78.2% at 1340 nm (Fig. 7b). PPBTQ had switching times of 0.75 s from the reduced to the oxidized state and 2.5 s from the oxidized to the reduced state at 336 nm, and in the NIR region (1340 nm), the response times were 2.35 s from the reduced to the oxidized state and 1.05 s from the oxidized to the reduced state. The dynamic electrochromic experiment for PPETQ film was carried out at 454 nm, 1430 nm and 1800 nm. The potential was interchanged between -0.2 V and 1.2 V at regular intervals of 5 s. The $\Delta T\%$ of the PPETQ was calculated to be 31.8 % at 454 nm, 77.6 % at 1430 nm and 80.3 % at 1800 nm, as shown in Fig. 7c. The response times of PPETQ were 1.45 s from the reduced to the oxidized state and 2.63 s from the oxidized to the reduced state at 454 nm, 1.83 s from the reduced to the oxidized state and 1.74 s from the oxidized to the reduced state at 1430 nm, 0.78 s from the reduced to the oxidized state and 1.25 s from the oxidized to the reduced state at 1800 nm. As to the difference in the response times at different wavelengths for each polymer film, it is probably due to the different switching modes at different wavelengths between the doping and dedoping process. From the data, it can be that PPETQ has better stability and higher percent transmittance contrast than that of PPTQ and PPBTQ after regular switching during 300 s clearly. PPBTQ and PPETQ have outstanding optical contrasts in the NIR region,

which is a very significant property for various NIR applications, such as for polymer based field-effect transistor and for camouflage device.

The coloration efficiency (*CE*) is also an important characteristic for the electrochromic materials. *CE* can be calculated by using the equations and given below [35]:

$$\Delta OD = \log\left(\frac{T_b}{T_c}\right) \quad \text{and} \quad \eta = \frac{\Delta OD}{\Delta Q}$$

where T_b and T_c are the transmittances before and after coloration, respectively. ΔOD is the change of the optical density, which is proportional to the amount of created color centers. η denotes the coloration efficiency (*CE*). ΔQ is the amount of injected charge per unit sample area. Using the equations mentioned above, the value of CE was measured as 252.4 cm^2 C^{-1} at 1230 nm for PPTQ. And the film PPBTQ was measured as 192.9 cm^2 C^{-1} at 336 nm and 402.9 cm^2 C^{-1} at 1340 nm. For PPETQ, the data were 114.2 cm^2 C^{-1} at 454 nm, 202.8 cm^2 C^{-1} at 1430 nm and 202.3 cm^2 C^{-1} at 1800 nm. These values are comparable with some newly reported D-A type polymers derived from quinoxaline derivatives[36]. Based on the above discussions, the distinct optical contrast, fast switching times and satisfactory *CE* values make three polymer films promising electrochromic materials in smart windows, especially in case of PPETQ.
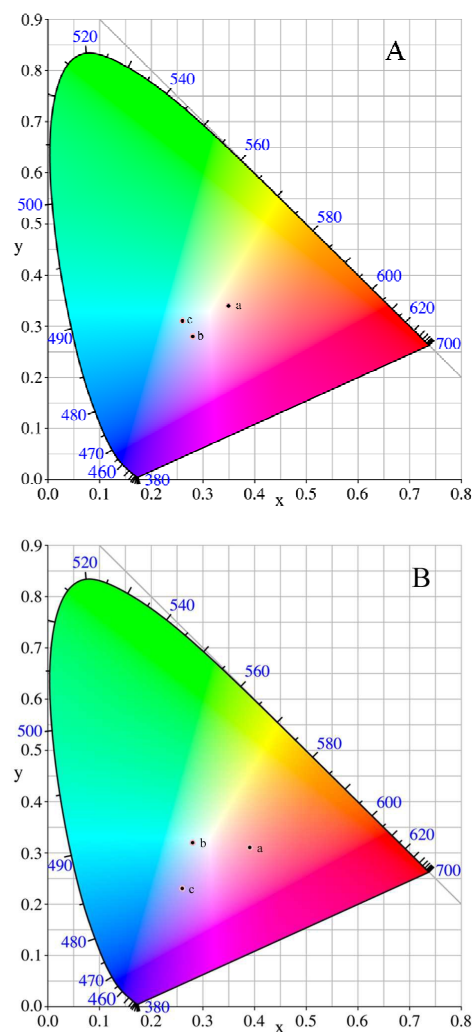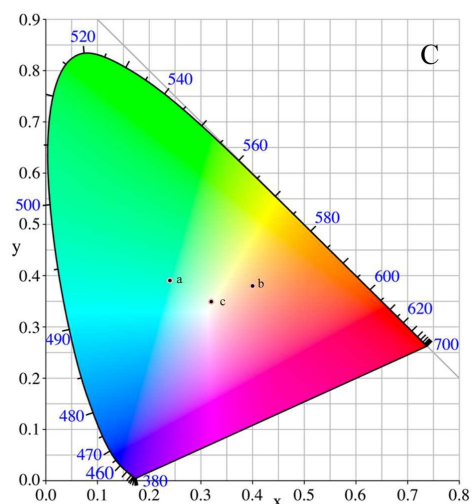
Fig. 6. Calculated colour trajectory in the CIE 1931 colour space for (A) PPTQ (a, -1.4 V; b, 0 V; c, 1.4 V), (B) PPBTQ (a, -1.5 V; b, 0 V; c, 1.4 V), and (C) PPETQ (a, -1.4 V; b, -0.2 V; c, 1.2 V) films deposited onto ITO/glass.
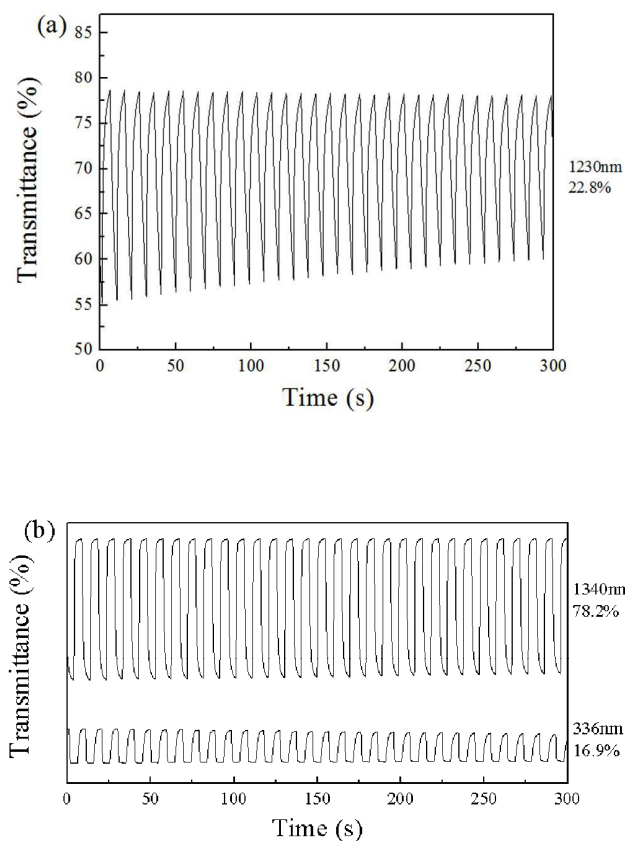

Fig. 7. Electrochromic switching under an applied square voltage signal for (a) PPTQ at 1230 nm, (b) PPBTQ at 336,1340 nm, and (c) PPETQ at 454, 1430 and 1800 nm with a residence time of 5 s.

Conclusions

In this study, three monomers based on 2,3-di(2-pyridyl) quinoxaline as the acceptor unit and three thiophene derivatives as the donor units were synthesized to understand the effects of electron-donating abilities of the donor unit on the electrochemical and spectroelectrochemical properties of the resulting electropolymerized materials. Due to the stronger electron donating ability of the 3,4-ethylenedioxythiophene unit, the 2,3-di(2-pyridyl)-5,8-bis(2-(3,4-ethylenedioxythienyl)) quinoxaline monomer has the lowest onset oxidation potential and the resultant poly[2,3-di(2-pyridyl)-5,8-bis(2-(3,4-ethylenedioxythienyl)) quinoxaline] has the lowest band gap. To the best of our knowledge, this is the first example of electropolymerized materials, poly[2,3-di(2-pyridyl)-5,8-bis(2-(3,4-ethylenedioxythienyl)) quinoxaline] exhibits a green color in the reduced state, yellow color in the neutral state, and colorless highly transmissive state in the oxidation state. As the donor-acceptor-donor type of π-conjugated polymers, they all showed high optical contrasts ($\Delta T\%$), fast response times and excellent cyclic voltammetry stabilities. What's more, generation of redox waves in CV at negative potentials and variation of the spectral absorption curves upon reduction proved that all three polymers have stable n-doping properties. The polymer films with their excellent electrochemical and optical properties, are expected to be useful for practical use in electrochromic display applications.

Acknowledgements

Appendix A. Supporting Information

Supplementary data associated with this article was attached with the manuscript.

[1]Department of Chemical Engineering, China University of Petroleum (East China), QingDao, 266580, P. R. China

[2]Shandong Key Laboratory of Chemical Energy Storage and Novel Cell Technology, Liaocheng University, Liaocheng, 252059, P. R. China

Corresponding author, Tel: +86-635-8539607; Fax: +86-635-8539607.

E-mail address: j.s.zhao@163.com (j.s.zhao);

Notes and references

1   E.C. Rios, A.V. Rosario, A. F. Nogueira, L. Micaronic, *Sol Energy Mater Sol Cell*, 2010, **94**, 1338-1345.

2   J. Huang, X. Wang, A. J. deMello, J. C. deMello, D. D. C. Bradley, *J. Mater. Chem*., 2007, **17**, 3551-3554.

3   Y. J. Zhang, K. Wang, G.L. Zhuang, Z.Q. Xie, C. Zhang, F. Cao, G.X. Pan, H.F. Chen, B. Zou, Y.G. Ma, *Chem. Eur. J*., **2015**, **21**, 2474-2479.

4   Y.J. Zhang, J.W. Sun, G.L. Zhuang, M. O.Y, Z.W.Yu, F. Cao, G.X. Pan, P.S. Tang, C. Zhang, Y.G. Ma, *J. Mater. Chem. C*, **2014**, **2**, 195-200.

5   C.M.Hangarter, M.Bangar, A. Mulchandania, N.V.Myung, *J. Mater. Chem*., 2010, **20**, 3131-3140.

6   K.R. Lee, G.A. Sotzing, *Chem. Commun.,* 2013, **49**, 5192-5194.

7   A. Cihaner, F. Algl, *Adv. Funct. Mater.,* 2008, **18**, 3583-3589.

8   C.M.Amb, A.L.Dyer, J.R.Reynolds, *Chem. Mater.*, 2011, **23**, 397-415.

9. G.E.Gunbas, A.Durmus, L. Toppare. *Adv. Mater.,* 2008, **20**, 691-695.

10 Z.Xu, M. Wang, J.S.Zhao, C.S.Cui, W.Y. Fan, J.F. Liu, *Electrochim. Acta.,* 2014, **125**, 241-249.

11 P.M.Beaujuge, S. Ellinger, J.R. Reynolds, *Nat. Mater.*, 2008, **7**, 795-799.

12 R.C.Coffin, J. Peet, J. Rogers, G.C. Bazan, *Nat. Chem.*, 2009, **1**, 657-661.

13 S.Hayashi, T.Koizumi, *Polym. Chem.*, 2012, **3**, 613-616.

14 D.M. Welsh, L.J. Kloeppner, L. Madrigal., M.R. Pinto., B.C. Thompson, K.S.Schanze., K.A.Abbound, D. Powell., J.R. Reynolds, *Macromolecules.*, 2002, **35**, 6517-6525.

15 A. Cirpan, A.A.Argun, C.R.G.Grenier, B.D. Reeves., J.R.Reynolds, *J . Mater. Chem*, 2013, **13**, 2422-2428.

16 A. Durmus, G.E.Gunbas, L. Toppare*, Chem. Mater.,* 2007, **19**, 6247-6251.

17 G.E.Gunbas, A. Durmus., L. Toppare, *Adv. Funct. Mater.,* 2008, **18**, 2026-2030.

18 E. Karabiyik, E. Sefer, F. B. Koyuncu, M. Tonga, E. Özdemir, S. Koyuncu. *Macromolecules.*, 2014, **47**, 8578-8584.

19 E.Sefer, S.O. Hacioglu, M. Tonga, L. Toppare, A. Cirpan, S. Koyuncu. *Macromol. Chem. Phys*., 2015, **216**, 829-836.

20 S.J.Chen, Y. Zhang, J.W. Gu, M.L. Ma, L. Zhang, J. Zhou, Y.Y. Zhou, *Express Polymer Letters*, 2012, **6** (6), 454-464.

21 Y. Tsubata, T. Suzuki, T. Miyashi, Y. Yamashita, *J. Org. Chem*., 1992, **57**, 6749-6755.

22 L. H. Xu, C. Su, C. Zhang, C. A. Ma, *Synth. Met*., 2011, **161**, 1856-1860.

23 E.M. Genies, G. Bidan, A.F. Diaz. *J. Electroanal. Chem*., 1983, **149**, 101-113.

24 S. Tarkuc, Y. A. Udum, L. Toppare, *Polymer.*, 2009,**50**, 3458-3464.

25 M. Ak, M.S. Ak, G. Kurtay, M. Güllü, L. Toppare, *Solid. State. Sci.*, 2010, **12**, 1199-1204.

26 H.T. Liu, Y.Z. Li, J.K. Xu , Z.G. Le, M.B. Luo, B.S. Wang, S.Z. Pu, L. Shen, *Eur. Polym. J .*, 2008, **44**, 171-188.

27 J. K. Xu, J. Hou, S. S. Zhang, Q. Xiao, R. Zhang, S. Z. Pu, and Q. L. Wei, *J. Phys. Chem. B*., 2006, **110**, 2643-2648.

28 D.M. de Leeuw, M.M.J. Simenon, A.R. Brown, R.E.F. Einerhand, *Synth. Met*., 1997, **87**, 53-59.

29 J. H. wang, J.I. Son, Y.B. Shim, *Sol. Energy. Mater. Sol. Cells*., 2010, **94**, 1286-1292.

30 W. Yang, J. S. Zhao, Y. Kong, T. Y. Kong, and C. S. Cui, *Int. J. Electrochem. Sci*., 2012, **7**, 2764-2780.

31 C.A. Thomas, K. Zong, K.A. Abboud, P.J. Steel, J.R. Reynolds, *J. Am. Chem. Soc.*, 2004, **126**, 50, 16440.

32 E. Yildiz, P. Camurlu, C. Tanyeli, I. Akhmedov, L. Toppare, *J. Electroanal. Chem.*, 2008, **612**, 247-256.

33 E. Sefer, F.B. Koyuncu, E. Oguzhan, S. Koyuncu., *J. Polym. Sci. Part A Polym. Chem*., 2010, **48**, 4419-4427.

34 B. Yigitsoy, S. Varis, C. Tanyeli, I.M. Akhmedov, L. Toppare., *Electrochim. Acta.*, 2007,**52**, 6561-6568.

35 S. J. Yoo, J. H. Cho, J. W. Lim, S. H. Park, J. Jang, Y.E. Sung, *Electrochem. Commun*., 2010, **12**, 164-167.

36 Y.X. Liu, M. Wang, J.S. Zhao, C.S. Cui, J.F. Liu, *RSC Adv*., 2014, 4, 52712-52726.

New Journal of Chemistry Accepted Manuscript

Donor–acceptor type polymers containing 2,3-bis(2-pyridyl)-5,8-dibromoquinoxaline acceptor and different thiophenes donors: Electrochemical, spectroelectrochemistry and electrochromic properties

Shuang Chen[1,2], Di Zhang[2], Min Wang[2], Lingqian Kong[2], Jinsheng Zhao[2*]
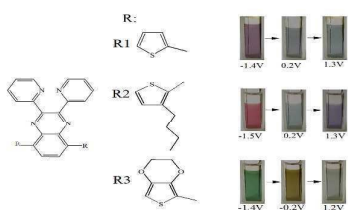
Three D-A type polymers were prepared, which showed desirable color switches, high optical contrasts, fast response time, high color efficiency.